

# Fermiophobic $Z'$ model for simultaneously explaining the muon anomalies $R_{K^{(*)}}$ and $(g-2)_\mu$

Mario Fernández Navarro<sup>\*</sup> and Stephen F. King<sup>†</sup>

*School of Physics & Astronomy, University of Southampton, SO17 1BJ Southampton, United Kingdom*

 (Received 3 December 2021; accepted 21 January 2022; published 14 February 2022)

We discuss a simple renormalizable, gauge invariant model with a fermiophobic  $Z'$  boson: it has no couplings to the three Standard Model (SM) chiral families, but does couple to a fourth vectorlike (VL) family. The SM Higgs couples to the fourth VL lepton, leading to an enhanced contribution to the muon anomalous magnetic moment  $(g-2)_\mu$ . The latter contribution requires a nonvanishing coupling of  $Z'$  to right-handed muons, which arises within this model due to mixing effects between the SM and VL fermions, along with  $Z'$  couplings to the second generation SM lepton doublet and third generation SM quark doublet. This model can simultaneously account for the measured  $B$ -decay ratios  $R_{K^{(*)}}$  and  $(g-2)_\mu$ . We identify the parameter space where this explanation is consistent with existing experimental constraints coming from  $B_s - \bar{B}_s$  mixing, neutrino trident production and collider searches. We also check that the SM Higgs coupling to the fourth VL lepton does not produce a dangerous contribution to the Higgs diphoton decay.

DOI: [10.1103/PhysRevD.105.035015](https://doi.org/10.1103/PhysRevD.105.035015)

## I. INTRODUCTION

Although the vast majority of particle-physics data is consistent with the predictions of the Standard Model (SM), in recent times a conspicuous series of discrepancies in flavor observables has been established. One example is the discrepancy in rare flavor-changing processes mediated by quark-level  $b(\bar{b}) \rightarrow s(\bar{s})\ell\bar{\ell}$  transitions, explored in the past by *BABAR* [1] and *Belle* [2], along with LHC [3,4]. In particular, the ratio of  $B$ -mesons decaying to  $K\ell^+\ell^-$ , which involves a  $\bar{b} \rightarrow \bar{s}\ell\bar{\ell}$  transition, has been recently measured by LHCb [5] in the dilepton mass-squared range  $1.1 < q^2 < 6 \text{ GeV}^2$  for the final states  $\mu^+\mu^-$  over  $e^+e^-$ ,

$$R_K^{[1.1,6]} = \frac{\text{Br}(B \rightarrow K\mu^+\mu^-)}{\text{Br}(B \rightarrow Ke^+e^-)} = 0.846_{-0.041}^{+0.044}, \quad (1)$$

along with the ratio of  $B$ -mesons decaying to  $K^*\ell^+\ell^-$ , measured in the past by LHCb [6],

$$R_{K^*}^{[1.1,6]} = \frac{\text{Br}(B \rightarrow K^*\mu^+\mu^-)}{\text{Br}(B \rightarrow K^*e^+e^-)} = 0.69_{-0.12}^{+0.16}. \quad (2)$$

Within the SM, lepton universality predicts  $R_{K^{(*)}} = 1$ , up to corrections of order 1% [7–11] due to the different mass of muons and electrons. Hence, the previous observations of  $R_{K^{(*)}}$  seem to indicate the breaking of SM lepton universality, up to the  $3.1\sigma$  [5] of the most updated measurement of  $R_K$ , while  $R_{K^*}$  is compatible with the SM expectations at  $2.4 - 2.5\sigma$  [6].

The apparent discrepancy of  $R_{K^{(*)}}$  with the SM may be a hint of new physics. Following these recent measurements of LHCb, a number of phenomenological analyses of this data, see, e.g., Refs. [12–24], favor new physics operators of the form  $\bar{s}_L\gamma_\mu b_L\bar{\mu}_L\gamma^\mu\mu_L$  or  $\bar{s}_L\gamma_\mu b_L\bar{\mu}_R\gamma^\mu\mu_R$ . In particular,  $R_{K^{(*)}}$  can be explained by only the purely left-handed (LH) operator with a coefficient  $\Lambda^{-2}$  where  $\Lambda \sim 40 \text{ TeV}$ , or also by a linear combination of both. Promising candidates for the arise of such effective operators are tree-level exchange of a hypothetical, electrically neutral and massive  $Z'$  boson (see, e.g., [25–30]) with nonuniversal couplings to SM fermions, or the contribution of a hypothetical leptoquark ( $LQ$ ) coupling with different strengths to the different types of charged leptons (see, e.g., [31–34]).

Independent of the  $R_{K^{(*)}}$  anomaly, there also exists a discrepancy with the SM predictions in the experimentally measured anomalous magnetic moments  $a = (g-2)/2$  of the muon and possibly the electron. The long-lasting noncompliance of the muon  $a_\mu$  with the SM was first observed by the Brookhaven E821 experiment at BNL [35].

<sup>\*</sup>M.F.Navarro@soton.ac.uk

<sup>†</sup>S.F.King@soton.ac.uk

*Published by the American Physical Society under the terms of the Creative Commons Attribution 4.0 International license. Further distribution of this work must maintain attribution to the author(s) and the published article's title, journal citation, and DOI. Funded by SCOAP<sup>3</sup>.*

This discrepancy has been recently confirmed by the most recent measurement of the Fermilab experiment [36],

$$\Delta a_\mu = a_\mu - a_\mu^{\text{SM}} = (2.51 \pm 0.59) \times 10^{-9}, \quad (3)$$

a result  $4.2\sigma$  greater than the SM prediction [37–57] and in excellent agreement with the previous BNL E821 measurement. Such a discrepancy can also be addressed by  $Z'$  models [58–66] or leptoquarks [67–69], along with models involving extended scalar content and/or vectorlike (VL) fermions [70–73]. In particular, the minimal  $Z'$  explanations [58] require to introduce  $\tau - \mu$  couplings in order to obtain an enhanced contribution proportional to  $m_\tau$ . In such models, dangerous contributions to the flavor-violating processes  $\tau \rightarrow 3\mu$  or  $\tau \rightarrow \mu\gamma$  may arise, along with possible breaking of lepton universality in leptonic tau decays, which is currently unobserved. Instead, Refs. [59–66] consider a fermiophobic  $Z'$  model where the  $Z'$  couplings with SM fermions are obtained through mixing with a 4th VL family. An enhanced contribution to  $\Delta a_\mu$  is obtained through a coupling between the SM Higgs and a 4th VL lepton, although it has to be checked that such a coupling would not spoil the existing Higgs diphoton decay data. Moreover, this contribution requires a nonvanishing coupling of  $Z'$  to right-handed (RH) muons, in such a way that a purely left-handed explanation of  $R_{K^{(*)}}$ , as in previous studies [29,30], cannot be performed in this case. The fact that the latest phenomenological analyses [23,24] leave the possibility to include an effective operator  $\bar{s}_L \gamma_\mu b_L \bar{\mu}_R \gamma^\mu \mu_R$  in the explanation of  $R_{K^{(*)}}$  opens the possibility to explain simultaneously  $R_{K^{(*)}}$  and  $(g-2)_\mu$  within this  $Z'$  model.

However, it has to be checked whether such simultaneous explanation of both anomalies can also preserve all currently released high energy experimental data, such as the measurement of the mass difference  $\Delta M_s$  of neutral  $B_s$  mesons, the observations of neutrino trident production and the most recent collider signatures. Ideally, such a model should be imminently testable with well-designed future searches. Moreover,  $U(1)'$  extensions of the SM can be affected by Landau poles well below the Planck scale, and in some cases only a few orders of magnitude above the TeV scale [74]. However, we consider here a bottom-up approach, where the  $U(1)'$  extension acts as an effective low energy theory, which would be embedded into a larger symmetry group below the energy scale of the Landau pole.

Regarding the electron  $g-2$ , there also exist measurements which suggest a possible discrepancy with the SM [75,76]. In [59], a similar  $Z'$  model was considered for addressing both the electron and muon  $g-2$ . It was concluded that it is not possible to address both anomalies simultaneously, mainly due to the strong bounds coming from  $\text{Br}(\mu \rightarrow e\gamma)$  and neutrino trident. The fermiophobic  $Z'$  model is a good candidate to explain either  $(g-2)_\mu$  or  $(g-2)_e$  (respecting all constraints) but not both simultaneously. Instead, in this article we will try to address both

$(g-2)_\mu$  and  $R_{K^{(*)}}$  simultaneously, which are insensitive to electrons, hence no prediction for  $(g-2)_e$  will be given.

There are other  $Z'$  models in the literature which address both anomalies by considering a 4th VL family. In [60] the couplings to muons are loop-induced, while the model in [61] contains an extra  $Z_1^{(1)} \times Z_2^{(2)}$  discrete symmetry and the  $Z'$  in [62,63] is not fermiophobic. The models in [64,65] are similar model to that considered here but with general mixing between VL and SM fermions, which leads to a large number of parameters, including all possible  $Z'$  couplings to SM fermion, along with dangerous FCNCs and  $Z - Z'$  kinetic mixing. Such a framework makes it difficult to systematically explore the parameter space, and instead a search of best fit points is performed. Moreover, such analyses reveal that the relevant parameters to simultaneously address  $R_{K^{(*)}}$  and  $(g-2)_\mu$  are only  $Z'$  couplings to  $bs$  quarks and muons. Hence, in contrast to the analyses in [64,65], in the present paper we consider a simplified  $Z'$  framework involving the fewest number of parameters in which the explanation of both anomalies can be simultaneously realized, allowing a systematic exploration of the parameter space.

The remainder of this article is organized as follows: in Sec. II we outline the renormalizable and gauge invariant fermiophobic model in which the  $Z'$  only couples to a vectorlike fourth family. In Sec. III, we show how it is possible to switch on the couplings of the  $Z'$  to the muon and  $bs$ -quarks through mixing with the VL fermions, thereby eliminating all unnecessary couplings and allowing us to focus on the connection between the  $R_{K^{(*)}}$  and  $(g-2)_\mu$  anomalies. The phenomenology and the constraints that affect this model are presented in Sec. IV. In Sec. V we

TABLE I. Particle assignments under  $SU(3)_c \times SU(2)_L \times U(1)_Y \times U(1)'$  gauge symmetry,  $i = 1, 2, 3$ . The singlet scalars  $\phi_f$  ( $f = Q, u, d, L, e, \nu$ ) have  $U(1)'$  charges  $-q_{f_4} = -q_{Q_4, u_4, d_4, L_4, e_4, \nu_4}$  [28].

| Field   | $SU(3)_c$ | $SU(2)_L$ | $U(1)_Y$ | $U(1)'$     |
|---|-----------|-----------|----------|-------------|
| $Q_{Li} = \begin{pmatrix} u_{Li} \\ d_{Li} \end{pmatrix}$   | <b>3</b>  | <b>2</b>  | 1/6      | 0           |
| $u_{Ri}$  | <b>3</b>  | <b>1</b>  | 2/3      | 0           |
| $d_{Ri}$  | <b>3</b>  | <b>1</b>  | -1/3     | 0           |
| $L_{Li} = \begin{pmatrix} \nu_{Li} \\ e_{Li} \end{pmatrix}$ | <b>1</b>  | <b>2</b>  | -1/2     | 0           |
| $e_{Ri}$  | <b>1</b>  | <b>1</b>  | -1       | 0           |
| $Q_{L4}, \tilde{Q}_{R4}$                                    | <b>3</b>  | <b>2</b>  | 1/6      | $q_{Q_4}$   |
| $u_{R4}, \tilde{u}_{L4}$                                    | <b>3</b>  | <b>1</b>  | 2/3      | $q_{u_4}$   |
| $d_{R4}, \tilde{d}_{L4}$                                    | <b>3</b>  | <b>1</b>  | -1/3     | $q_{d_4}$   |
| $L_{L4}, \tilde{L}_{R4}$                                    | <b>1</b>  | <b>2</b>  | -1/2     | $q_{L_4}$   |
| $e_{R4}, \tilde{e}_{L4}$                                    | <b>1</b>  | <b>1</b>  | -1       | $q_{e_4}$   |
| $\nu_{R4}, \tilde{\nu}_{L4}$                                | <b>1</b>  | <b>1</b>  | 0        | $q_{\nu_4}$ |
| $\phi_f$  | <b>1</b>  | <b>1</b>  | 0        | $-q_{f_4}$  |
| $H = \begin{pmatrix} h^+ \\ (v+h^0)/\sqrt{2} \end{pmatrix}$ | <b>1</b>  | <b>2</b>  | 1/2      | 0           |

systematically explore the parameter space of the model, and we also display and discuss the results from our analysis. Finally, Sec. VI concludes the article.

## II. THE MODEL

The model [28] (Table I) includes the three chiral families of left-handed (LH)  $SU(2)_L$  doublets  $(Q_{Li}, L_{Li})$  and right-handed (RH)  $SU(2)_L$  singlets  $(u_{Ri}, d_{Ri}, e_{Ri})$  of the SM,  $i = 1, 2, 3$ ; along with one vectorlike family of fermions (formed by LH and RH  $SU(2)_L$  doublets  $Q_{L4}, L_{L4}$ , and  $\tilde{Q}_{R4}, \tilde{L}_{R4}$ , together with LH and RH  $SU(2)_L$  singlets  $u_{R4}, d_{R4}, e_{R4}, \nu_{R4}$  and  $\tilde{u}_{L4}, \tilde{d}_{L4}, \tilde{e}_{L4}, \tilde{\nu}_{L4}$ ). The vectorlike fermions are charged under a gauge symmetry  $U(1)'$ , while

the three chiral families remain neutral under this symmetry, which is the reason behind the model being called fermiophobic. The scalar sector is augmented by gauge singlet fields  $\phi_f$  with nontrivial charge assignments  $-q_{f_4}$  under the new symmetry, which are responsible for spontaneously breaking  $U(1)'$  developing vacuum expectation values (VEVs)  $\langle \phi_f \rangle$ . The  $Z'$  boson generated after the symmetry breaking has a mass at the same scale  $\langle \phi_f \rangle$ . On the other hand, the vectorlike neutrino singlets would lead to the type Ib seesaw mechanism for generating the light neutrino masses, which was introduced in [77], although this is beyond the scope of this article.

The full renormalizable Lagrangian is

$$\begin{aligned} \mathcal{L}^{\text{ren}} = & y_{ij}^u \bar{Q}_{Li} \tilde{H} u_{Rj} + y_{ij}^d \bar{Q}_{Li} H d_{Rj} + y_{ij}^e \bar{L}_{Li} H e_{Rj} + y_4^u \bar{Q}_{L4} \tilde{H} u_{R4} + y_4^d \bar{Q}_{L4} H d_{R4} + y_4^e \bar{L}_{L4} H e_{R4} + y_4^\nu \bar{L}_{L4} \tilde{H} \nu_{R4} \\ & + x_i^Q \phi_Q \bar{Q}_{Li} \tilde{Q}_{R4} + x_i^L \phi_L \bar{L}_{Li} \tilde{L}_{R4} + x_i^u \phi_u^* \tilde{u}_{L4} u_{Ri} + x_i^d \phi_d^* \tilde{d}_{L4} d_{Ri} + x_i^e \phi_e^* \tilde{e}_{L4} e_{Ri} \\ & + M_4^Q \bar{Q}_{L4} \tilde{Q}_{R4} + M_4^L \bar{L}_{L4} \tilde{L}_{R4} + M_4^u \tilde{u}_{L4} u_{R4} + M_4^d \tilde{d}_{L4} d_{R4} + M_4^e \tilde{e}_{L4} e_{R4} + M_4^\nu \tilde{\nu}_{L4} \nu_{R4} + \text{H.c.} \end{aligned} \quad (4)$$

where  $\tilde{H} = i\sigma_2 H^*$ ,  $i = 1, 2, 3$ . The requirement of  $U(1)'$  invariance of the Yukawa interactions involving the fourth family yields the following constraints on the  $U(1)'$  charges:

$$q_{Q_4} = q_{u_4} = q_{d_4}, \quad q_{L_4} = q_{e_4} = q_{\nu_4}. \quad (5)$$

It is clear from Eq. (4) that fields in the 4th, vectorlike family obtain masses from two sources. Firstly, from Yukawa terms involving the SM Higgs field, such as  $y_4^e \bar{L}_{L4} H e_{R4}$ , which get promoted to chirality-flipping fourth family mass terms  $M_4^C$  once the SM Higgs acquires a VEV. Secondly, from vectorlike mass terms, like  $M_4^L \bar{L}_{L4} \tilde{L}_{R4}$ . For the purpose of clarity, we shall treat  $M_4^C$  and  $M_4^L$  as

independent masses in the analysis of the physical quantities of interest, rather than constructing the full fourth family mass matrix and diagonalizing it, since such quantities rely on a chirality flip and are sensitive to  $M_4^C$  rather than the vectorlike masses  $M_4^L$ . Spontaneous breaking of  $U(1)'$  by the scalars  $\phi_f$  spontaneously acquiring VEVs gives rise to a massive  $Z'$  boson featuring couplings with the vectorlike fermion fields. In the interaction basis such terms will be diagonal and of the following form:

$$\begin{aligned} \mathcal{L}_{Z'}^{\text{gauge}} = & g' Z'_\mu (\bar{Q}_L D_Q \gamma^\mu Q_L + \bar{u}_R D_u \gamma^\mu u_R + \bar{d}_R D_d \gamma^\mu d_R \\ & + \bar{L}_L D_L \gamma^\mu L_L + \bar{e}_R D_e \gamma^\mu e_R + \bar{\nu}_R D_\nu \gamma^\mu \nu_R), \end{aligned} \quad (6)$$

where

$$\begin{aligned} D_Q = \text{diag}(0, 0, 0, q_{Q_4}), \quad D_u = \text{diag}(0, 0, 0, q_{Q_4}), \quad D_d = \text{diag}(0, 0, 0, q_{Q_4}), \\ D_L = \text{diag}(0, 0, 0, q_{L_4}), \quad D_e = \text{diag}(0, 0, 0, q_{L_4}), \quad D_\nu = \text{diag}(0, 0, 0, q_{L_4}). \end{aligned} \quad (7)$$

At this stage, the SM quarks and leptons do not couple to the  $Z'$ . However, the Yukawa couplings detailed in Eq. (4) have no requirement to be diagonal. Before we can determine the full masses of the propagating vectorlike states and SM fermions, we need to transform the field content of the model such that the Yukawa couplings become diagonal. Therefore, fermions in the mass basis (denoted by primed fields) are related to particles in the interaction basis by the following unitary transformations

$$\begin{aligned} Q'_L = V_{Q_L} Q_L, \quad u'_R = V_{u_R} u_R, \quad d'_R = V_{d_R} d_R, \\ L'_L = V_{L_L} L_L, \quad e'_R = V_{e_R} e_R, \quad \nu'_R = V_{\nu_R} \nu_R. \end{aligned} \quad (8)$$

This mixing induces couplings of SM mass eigenstate fermions to the massive  $Z'$ , which can be expressed as follows

$$\begin{aligned} D'_Q = V_{Q_L} D_Q V_{Q_L}^\dagger, \quad D'_u = V_{u_R} D_u V_{u_R}^\dagger, \quad D'_d = V_{d_R} D_d V_{d_R}^\dagger, \\ D'_L = V_{L_L} D_L V_{L_L}^\dagger, \quad D'_e = V_{e_R} D_e V_{e_R}^\dagger, \quad D'_\nu = V_{\nu_R} D_\nu V_{\nu_R}^\dagger. \end{aligned} \quad (9)$$

## III. MIXING

In this article, we consider a minimal mixing framework<sup>1</sup> in which both anomalies  $R_{K^{(*)}}$  and  $(g-2)_\mu$  can be

simultaneously addressed. This requires that the 4th VL fermion family mixes only with the third generation of the SM quark doublet and with the second generation of the SM lepton doublet and singlet,

$$V_{Q_L} = V_{34}^{Q_L}, \quad V_{L_L} = V_{24}^{L_L}, \quad V_{e_R} = V_{24}^{e_R}, \quad (10)$$

where

$$V_{34}^{Q_L} = \begin{pmatrix} 1 & 0 & 0 & 0 \\ 0 & 1 & 0 & 0 \\ 0 & 0 & \cos \theta_{34}^Q & \sin \theta_{34}^Q \\ 0 & 0 & -\sin \theta_{34}^Q & \cos \theta_{34}^Q \end{pmatrix}, \quad (11)$$

$$V_{24}^{L_L, e_R} = \begin{pmatrix} 1 & 0 & 0 & 0 \\ 0 & \cos \theta_{24}^{L_L, e_R} & 0 & \sin \theta_{24}^{L_L, e_R} \\ 0 & 0 & 1 & 0 \\ 0 & -\sin \theta_{24}^{L_L, e_R} & 0 & \cos \theta_{24}^{L_L, e_R} \end{pmatrix}, \quad (12)$$

so for the matrices in Eq. (9) we obtain

$$D'_Q = V_{34}^{Q_L} D_Q (V_{34}^{Q_L})^\dagger \\ = q_{Q_4} \begin{pmatrix} 0 & 0 & 0 & 0 \\ 0 & 0 & 0 & 0 \\ 0 & 0 & (\sin \theta_{34}^Q)^2 & \cos \theta_{34}^Q \sin \theta_{34}^Q \\ 0 & 0 & \cos \theta_{34}^Q \sin \theta_{34}^Q & (\cos \theta_{34}^Q)^2 \end{pmatrix}, \quad (13)$$

$$D'_L = V_{24}^{L_L} D_L (V_{24}^{L_L})^\dagger \\ = q_{L_4} \begin{pmatrix} 0 & 0 & 0 & 0 \\ 0 & (\sin \theta_{24}^{L_L})^2 & 0 & \cos \theta_{24}^{L_L} \sin \theta_{24}^{L_L} \\ 0 & 0 & 0 & 0 \\ 0 & \cos \theta_{24}^{L_L} \sin \theta_{24}^{L_L} & 0 & (\cos \theta_{24}^{L_L})^2 \end{pmatrix}, \quad (14)$$

$$D'_e = V_{24}^{e_R} D_e (V_{24}^{e_R})^\dagger \\ = q_{L_4} \begin{pmatrix} 0 & 0 & 0 & 0 \\ 0 & (\sin \theta_{24}^{e_R})^2 & 0 & \cos \theta_{24}^{e_R} \sin \theta_{24}^{e_R} \\ 0 & 0 & 0 & 0 \\ 0 & \cos \theta_{24}^{e_R} \sin \theta_{24}^{e_R} & 0 & (\cos \theta_{24}^{e_R})^2 \end{pmatrix}, \quad (15)$$

hence in this basis the relevant  $Z'$  couplings read

$$\mathcal{L}_{Z'} \supset Z'_\mu (g_{bb} \bar{b}_L \gamma^\mu b_L + g_{\mu\mu}^L \bar{\mu}_L \gamma^\mu \mu_L + g_{\mu\mu}^R \bar{\mu}_R \gamma^\mu \mu_R), \quad (16)$$

where

<sup>1</sup>Such a simplified mixing framework could be enforced by introducing some family symmetry, however a discussion of this is beyond the scope of this article.

$$g_{bb} = g' q_{Q_4} (\sin \theta_{34}^Q)^2, \quad (17)$$

$$g_{\mu\mu}^L = g' q_{L_4} (\sin \theta_{24}^{L_L})^2, \quad (18)$$

$$g_{\mu\mu}^R = g' q_{L_4} (\sin \theta_{24}^{e_R})^2. \quad (19)$$

We also obtain a CKM suppressed  $bs$  coupling in the basis in which the up-quark mass matrix is diagonal. In this basis,  $V_{\text{CKM}} = V_{d_L}^\dagger$ , and we find the couplings

$$Z' g_{bs} \bar{s}_L \gamma^\mu b_L, \quad (20)$$

where

$$g_{bs} = g_{bb} V_{ts} = g' q_{Q_4} (\sin \theta_{34}^Q)^2 V_{ts}, \quad (21)$$

and  $V_{ts} \approx -0.04$ . Usually  $R_{K^{(*)}}$  can be addressed with just  $g_{bs}$  and  $g_{\mu\mu}^L$  couplings (see, e.g., [28–30]), but we also need  $g_{\mu\mu}^R$  in order to simultaneously explain  $(g-2)_\mu$  in this model, as we shall see in the next section. Moreover, here both anomalies  $R_{K^{(*)}}$  and  $(g-2)_\mu$  are insensitive to electrons and taus, hence the electron and tau related  $Z'$  couplings and mixing angles are free parameters. Therefore, no prediction is given in this model for decays with taus like  $B \rightarrow K^{(*)} \tau \bar{\tau}$  and other LFV processes like  $\Upsilon \rightarrow \tau \mu$ . This is different from other  $Z'$  models such as [58], where  $Z'$  couplings with taus are involved in the explanation of  $(g-2)_\mu$ .

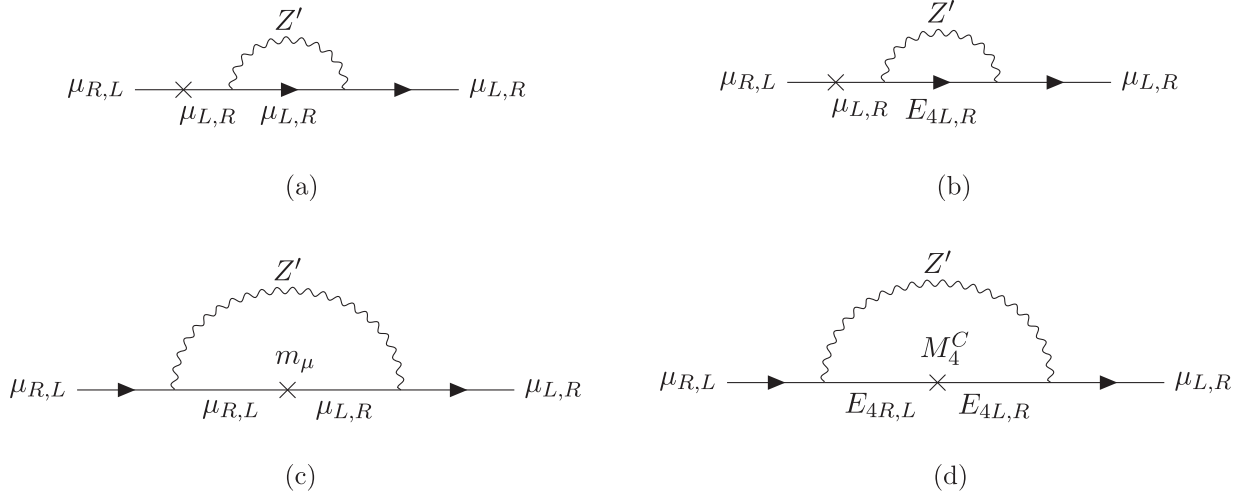
## IV. PHENOMENOLOGY AND FLAVOR CONSTRAINTS

### A. $(g-2)_\mu$

The diagrams displayed in Fig. 1 lead to  $Z'$ -mediated contributions to the muon anomalous magnetic moment, namely [59]

$$\Delta a_\mu = -\frac{m_\mu^2}{8\pi^2 M_{Z'}^2} \left[ (|g_{\mu\mu}^L|^2 + |g_{\mu\mu}^R|^2) F(m_\mu^2/M_{Z'}^2) \right. \\ + (|g_{\mu E}^L|^2 + |g_{\mu E}^R|^2) F(m_E^2/M_{Z'}^2) \\ + \text{Re}[g_{\mu\mu}^L (g_{\mu\mu}^R)^*] G(m_\mu^2/M_{Z'}^2) \\ \left. + \text{Re}[g_{\mu E}^L (g_{\mu E}^R)^*] \frac{M_4^C}{m_\mu} G(m_E^2/M_{Z'}^2) \right], \quad (22)$$

where  $G(x)$  and  $F(x)$  are  $\mathcal{O}(1)$  loop functions, and  $m_E$  is the propagating mass of the 4th lepton. In our case,  $m_E \simeq M_4^L$  since we consider that the dominant source of mass for the 4th lepton is vectorlike, i.e.,  $M_4^L \gg M_4^C$ . For the upcoming sections we shall fix  $M_4^L = 5$  TeV, in order to preserve  $M_4^L \gg M_4^C$  for a chirality-flipping mass  $M_4^C$  of order GeV. The couplings between muons and VL leptons read


 FIG. 1. Feynman diagrams in the model contributing to  $(g-2)_\mu$ , photon lines are implicit.

$$\begin{aligned}
 g_{\mu E}^L &= g' q_{L4} \cos \theta_{24}^{L4} \sin \theta_{24}^{L4} \\
 &= g' q_{L4} \sqrt{1 - g_{\mu\mu}^L / (g' q_{L4})} \sqrt{g_{\mu\mu}^L / (g' q_{L4})}, \quad (23)
 \end{aligned}$$

$$\begin{aligned}
 g_{\mu E}^R &= g' q_{L4} \cos \theta_{24}^{eR} \sin \theta_{24}^{eR} \\
 &= g' q_{L4} \sqrt{1 - g_{\mu\mu}^R / (g' q_{L4})} \sqrt{g_{\mu\mu}^R / (g' q_{L4})}, \quad (24)
 \end{aligned}$$

where from now on we will assume  $g' q_{L4} = 1$  for simplicity.

Since the loop functions satisfy  $G(x) < 0$  and  $F(x) > 0$ , the contributions proportional to  $G(x)$  and  $F(x)$  in Eq. (22) interfere negatively. However, for a chirality-flipping mass  $M_4^C$  of order  $v/\sqrt{2}$  (where  $v = 246$  GeV is the SM Higgs VEV), the term proportional to  $M_4^C$  in Eq. (22) is dominant and positive due to  $G(x) < 0$ , matching the required sign to explain the experimental measurement of  $\Delta a_\mu$  by Fermilab [36] [see Eq. (3)]. Hence, a nonvanishing coupling of  $Z'$  to RH muons is crucial to explain  $(g-2)_\mu$  here: otherwise, if we assume  $g_{\mu\mu}^R = 0$ , then  $g_{\mu E}^R$  vanishes and we lose the dominant contribution proportional to  $M_4^C$ .

### B. $R_{K^{(*)}}$

One possible explanation of the  $R_{K^{(*)}}$  measurements in LHCb is that the low-energy Lagrangian below the EW scale contains additional contributions to the effective 4-fermion operator with left/right-handed muon, left-handed  $b$ -quark, and left-handed  $s$ -quark fields,

$$\begin{aligned}
 \Delta \mathcal{L}_{\text{eff}} \supset & G_{bs\mu}^L (\bar{s}_L \gamma_\mu b_L) (\bar{\mu}_L \gamma^\mu \mu_L) \\
 & + G_{bs\mu}^R (\bar{s}_L \gamma_\mu b_L) (\bar{\mu}_R \gamma^\mu \mu_R) + \text{H.c.}, \quad (25)
 \end{aligned}$$

arising in our model from integrating out the  $Z'$  boson at tree-level [Fig. 2(a)]. The above operators contribute to the flavor changing transitions  $b_L \rightarrow s_L \bar{\mu}_L \mu_L$  and

$b_L \rightarrow s_L \bar{\mu}_R \mu_R$ , respectively. A  $Z'$ -mediated contribution to  $B_s \rightarrow \bar{\mu} \mu$  [Fig. 2(c)] also arises.

We can express the coefficients  $G_{bs\mu}^L$  and  $G_{bs\mu}^R$  as a function of the couplings  $g_{bb}$ ,  $g_{\mu\mu}^L$ , and  $g_{\mu\mu}^R$ ,

$$G_{bs\mu}^L = -\frac{V_{ts} g_{bb} g_{\mu\mu}^L}{M_{Z'}^2} = \frac{-V_{ts} (g')^2 q_{Q4} q_{L4} (\sin \theta_{34}^Q)^2 (\sin \theta_{24}^{L4})^2}{M_{Z'}^2}, \quad (26)$$

$$G_{bs\mu}^R = -\frac{V_{ts} g_{bb} g_{\mu\mu}^R}{M_{Z'}^2} = \frac{-V_{ts} (g')^2 q_{Q4} q_{L4} (\sin \theta_{34}^Q)^2 (\sin \theta_{24}^{eR})^2}{M_{Z'}^2}, \quad (27)$$

where it can be seen that both  $G_{bs\mu}^L$  and  $G_{bs\mu}^R$  have the same sign in our model.

In Ref. [24], the vector and axial effective operators

$$\begin{aligned}
 \mathcal{H}_{\text{eff}} \supset & \mathcal{N} [\delta C_9 (\bar{s}_L \gamma_\mu b_L) (\bar{\mu} \gamma^\mu \mu) \\
 & + \delta C_{10} (\bar{s}_L \gamma_\mu b_L) (\bar{\mu} \gamma^\mu \gamma_5 \mu)] + \text{H.c.}, \quad (28)
 \end{aligned}$$

$$\mathcal{N} = -\frac{4G_F}{\sqrt{2}} V_{tb} V_{ts}^* \frac{e^2}{16\pi^2}, \quad (29)$$

had been fitted to explain  $R_{K^{(*)}}$  up to the  $1\sigma$  level, as shown in Tables II and III. From the results for  $\delta C_9$  and  $\delta C_{10}$  we have computed the numerical values of  $G_{bs\mu}^L$  and  $G_{bs\mu}^R$  that fit  $R_{K^{(*)}}$  up to the  $1\sigma$  level,

$$\delta C_9 = -\frac{G_{bs\mu}^L + G_{bs\mu}^R}{2\mathcal{N}} \Rightarrow G_{bs\mu}^L = \mathcal{N} (\delta C_{10} - \delta C_9), \quad (30)$$

$$\delta C_{10} = \frac{G_{bs\mu}^L - G_{bs\mu}^R}{2\mathcal{N}} \Rightarrow G_{bs\mu}^R = -\mathcal{N} (\delta C_9 + \delta C_{10}). \quad (31)$$

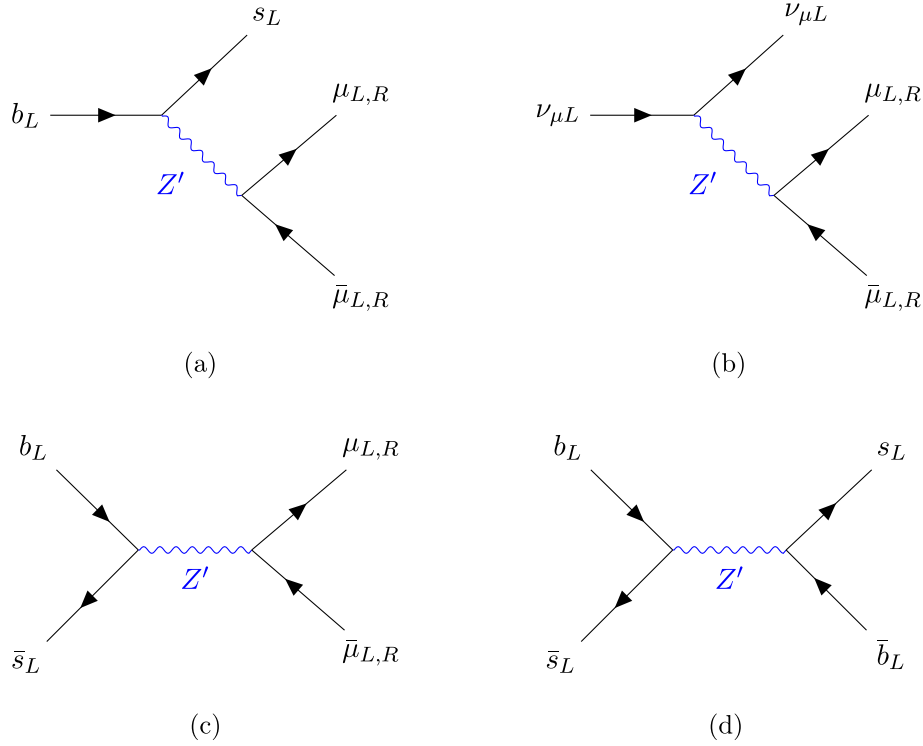


FIG. 2. (a)  $Z'$  exchange diagrams contributing to  $R_{K^{(*)}}$ . (b)  $Z'$  exchange diagrams contributing to neutrino trident production. (c)  $Z'$  exchange diagrams contributing to  $B_s \rightarrow \bar{\mu}\mu$ . (d)  $Z'$  exchange diagrams contributing to  $B_s - \bar{B}_s$  mixing.

The results displayed in Table II consider the so-called “theoretically clean fit” which, as explained in Ref. [24], displays the values of  $G_{bs\mu}^L$  and  $G_{bs\mu}^R$  that simultaneously fit  $R_{K^{(*)}}$  and the  $B_s \rightarrow \bar{\mu}\mu$  data. This fit is denoted as theoretically clean since all the observables included are free from theoretical uncertainties. On the other hand, the global fit in Table III also includes the fit of angular observables in  $B \rightarrow K^* \bar{\mu}\mu$  data reported by LHCb, ATLAS and CMS, which are afflicted by larger theoretical

uncertainties than the ratios of lepton universality violation and the  $B_s \rightarrow \bar{\mu}\mu$  data [24].

On one hand,  $G_{bs\mu}^L$  shows similar best fit values of order  $(40 \text{ TeV})^{-2}$  in both fits, although the  $1\sigma$  region is slightly tighter in the global fit (Table III) than in the theoretically clean fit (Table II). On the other hand,  $G_{bs\mu}^R$  shows the largest differences between both fits. For the theoretically clean fit,  $G_{bs\mu}^R < 0$  is favored, although  $G_{bs\mu}^R > 0$  is still allowed. For the global fit, the situation is the opposite:

TABLE II. Fit of  $R_{K^{(*)}}$  and the  $B_s \rightarrow \bar{\mu}\mu$  data (theoretically clean fit) [24].

|  | Best fit   | $1\sigma$ range   |
|--|--|---|
| $(\delta C_9, \delta C_{10})$                        | $(-0.11, 0.59)$  | $\delta C_9 \in [-0.41, 0.17], \delta C_{10} \in [0.38, 0.81]$  |
| $(G_{bs\mu}^L/\mathcal{N}, G_{bs\mu}^R/\mathcal{N})$ | $(0.7, -0.48)$   | $G_{bs\mu}^L/\mathcal{N} \in [0.64, 0.79], G_{bs\mu}^R/\mathcal{N} \in [-0.98, 0.03]$   |
| $(G_{bs\mu}^L, G_{bs\mu}^R)$                         | $\left(\frac{1}{(42.5 \text{ TeV})^2}, -\frac{1}{(51.3 \text{ TeV})^2}\right)$ | $G_{bs\mu}^L \in \left[\frac{1}{(44.44 \text{ TeV})^2}, \frac{1}{(40 \text{ TeV})^2}\right], G_{bs\mu}^R \in \left[-\frac{1}{(35.9 \text{ TeV})^2}, \frac{1}{(205 \text{ TeV})^2}\right]$ |

TABLE III. Fit of  $R_{K^{(*)}}$ ,  $B_s \rightarrow \bar{\mu}\mu$  data and angular observables of  $B \rightarrow K^* \bar{\mu}\mu$  data (global fit) [24].

|  | Best fit  | $1\sigma$ range  |
|--|---|--|
| $(\delta C_9, \delta C_{10})$                        | $(-0.56, 0.30)$   | $\delta C_9 \in [-0.79, -0.31], \delta C_{10} \in [0.15, 0.49]$  |
| $(G_{bs\mu}^L/\mathcal{N}, G_{bs\mu}^R/\mathcal{N})$ | $(0.86, 0.26)$  | $G_{bs\mu}^L/\mathcal{N} \in [0.8, 0.94], G_{bs\mu}^R/\mathcal{N} \in [-0.18, 0.64]$   |
| $(G_{bs\mu}^L, G_{bs\mu}^R)$                         | $\left(\frac{1}{(38.34 \text{ TeV})^2}, \frac{1}{(69.73 \text{ TeV})^2}\right)$ | $G_{bs\mu}^L \in \left[\frac{1}{(39.75 \text{ TeV})^2}, \frac{1}{(36.67 \text{ TeV})^2}\right], G_{bs\mu}^R \in \left[-\frac{1}{(83.8 \text{ TeV})^2}, \frac{1}{(44.44 \text{ TeV})^2}\right]$ |

$G_{bs\mu}^R > 0$  is favored, although  $G_{bs\mu}^R < 0$  is also allowed. As a consequence, in both fits  $G_{bs\mu}^R$  is compatible with zero and hence  $R_{K^{(*)}}$  can also be explained with only the purely left-handed operator  $\bar{s}_L\gamma_\mu b_L\bar{\mu}_L\gamma^\mu\mu_L$ , as in previous  $Z'$  models [28–30]. However, we have shown that we need a non-vanishing coupling of right-handed muons to  $Z'$  in order to explain  $(g-2)_\mu$ , hence within this model we have a nonzero right-handed contribution to  $R_{K^{(*)}}$ . Therefore, we need to be aware of keeping such contribution, i.e.,  $G_{bs\mu}^R$ , within the  $1\sigma$  region of the considered fit.

Moreover, the best fit value of  $G_{bs\mu}^R$  is negative within the theoretically clean fit, but positive within the global fit. This indicates that the extra angular observables of  $B \rightarrow K^*\bar{\mu}\mu$  data are relevant and drastically change the picture for explaining  $R_{K^{(*)}}$  with effective operators  $\bar{s}_L\gamma_\mu b_L\bar{\mu}_R\gamma^\mu\mu_R$ . However, the fact that these angular observables are affected by important theoretical uncertainties lead to some tension in the community about whether angular observables of  $B \rightarrow K^*\bar{\mu}\mu$  data should be considered or not in the global fits. Because of this, during the remainder of this work we will consider both fits for computing our results. On the other hand, in our model  $G_{bs\mu}^L$  and  $G_{bs\mu}^R$  must have the same relative sign. Therefore, we shall keep the product  $q_{Q_4}q_{L4}$  positive and then fit  $G_{bs\mu}^R$  in the positive region allowed within the  $1\sigma$ . We shall study whether this can be challenging in the theoretically clean fit, where the positive region allowed by the  $1\sigma$  range of  $G_{bs\mu}^R$  is tiny. In other words, the requirement of keeping  $G_{bs\mu}^R$  within the  $1\sigma$  range of the theoretically clean fit constitutes an extra effective constraint over this model.

### C. $B_s - \bar{B}_s$ mixing

The  $Z'$  coupling to  $bs$ -quarks in Eq. (20) leads to an additional tree-level contribution [Fig. 2(d)] to  $B_s - \bar{B}_s$  mixing,

$$\Delta\mathcal{L}_{\text{eff}} \supset -\frac{G_{bs}}{2}(\bar{s}_L\gamma^\mu b_L)^2 + \text{H.c.} \quad (32)$$

where

$$G_{bs} = \frac{g_{bs}^2}{M_{Z'}^2} = \frac{g_{bb}^2 V_{ts}^2}{M_{Z'}^2}. \quad (33)$$

Such a new contribution is constrained by the results of the mass difference  $\Delta M_s$  of neutral  $B_s$  mesons. The theoretical determination of the mass difference is limited by our understanding of nonperturbative matrix elements of dimension six operators, which can be computed with lattice simulations or sum rules. Here we follow the recent analysis of Ref. [78], which displays two different results for  $\Delta M_s$ ,

$$\Delta M_s^{\text{FLAG}/19} = (1.13_{-0.07}^{+0.07})\Delta M_s^{\text{exp}}, \quad (34)$$

$$\Delta M_s^{\text{Average}/19} = (1.04_{-0.09}^{+0.04})\Delta M_s^{\text{exp}}. \quad (35)$$

$\Delta M_s^{\text{FLAG}/19}$  is obtained using lattice results, and is about two standard deviations above the experimental numbers. This result for the mass difference sets the strong bound

$$G_{bs} \lesssim \frac{1}{(330 \text{ TeV})^2}. \quad (36)$$

On the other hand,  $\Delta M_s^{\text{Average}/19}$ , obtained as a weighted average from both lattice simulations and sum rule results, shows better agreement with the experiment, and a reduction of the total errors by about 40%. This result for the mass difference sets a less constraining bound

$$G_{bs} \lesssim \frac{1}{(220 \text{ TeV})^2}. \quad (37)$$

The resulting constraints will be shown as blue regions over the parameter space.

### D. Neutrino trident

The  $Z'$  couplings to the second generation of the SM lepton doublet and singlet lead to a new tree-level contribution [Fig. 2(b)] to the effective 4-lepton interaction

$$\begin{aligned} \Delta\mathcal{L}_{\text{eff}} \supset & -\frac{(g_{\mu\mu}^L)^2}{2M_{Z'}^2}(\bar{\mu}_L\gamma_\mu\mu_L)(\bar{\nu}_{\mu L}\gamma^\mu\nu_{\mu L}) \\ & -\frac{g_{\mu\mu}^R g_{\mu\mu}^L}{M_{Z'}^2}(\bar{\mu}_R\gamma_\mu\mu_R)(\bar{\nu}_{\mu L}\gamma^\mu\nu_{\mu L}). \end{aligned} \quad (38)$$

This operator is constrained by the trident production  $\nu_\mu\gamma^* \rightarrow \nu_\mu\mu^+\mu^-$  [81–83]. Using the results of the global fit in Ref. [79], the bound over  $g_{\mu\mu}^L$  and  $g_{\mu\mu}^R$  is given by

$$-\frac{1}{(390 \text{ GeV})^2} \lesssim \frac{(g_{\mu\mu}^L)^2 + g_{\mu\mu}^L g_{\mu\mu}^R}{M_{Z'}^2} \lesssim \frac{1}{(370 \text{ GeV})^2}, \quad (39)$$

whereas in our case only the right side of (39) applies, since according to Eqs. (18) and (19)  $g_{\mu\mu}^L$  and  $g_{\mu\mu}^R$  have the same relative sign in our model and hence the product  $g_{\mu\mu}^L g_{\mu\mu}^R$  is positive. The resulting constraints will be shown as orange regions over the parameter space.

### E. Constraints from lepton flavor violation

Within the lepton sector the  $Z'$  only couples to muons, hence no  $Z'$  lepton flavor-violating couplings are generated. Therefore, in our  $Z'$  model there are no contributions to lepton flavor-violating processes such as  $\mu \rightarrow e\gamma$  or  $\tau \rightarrow 3\mu$ .

### F. Collider constraints

Our model is not constrained by electron collider searches since our  $Z'$  does not couple to electrons. However, further constraints on our model come from LHC searches. For light  $Z'$  masses, the LHC measurements

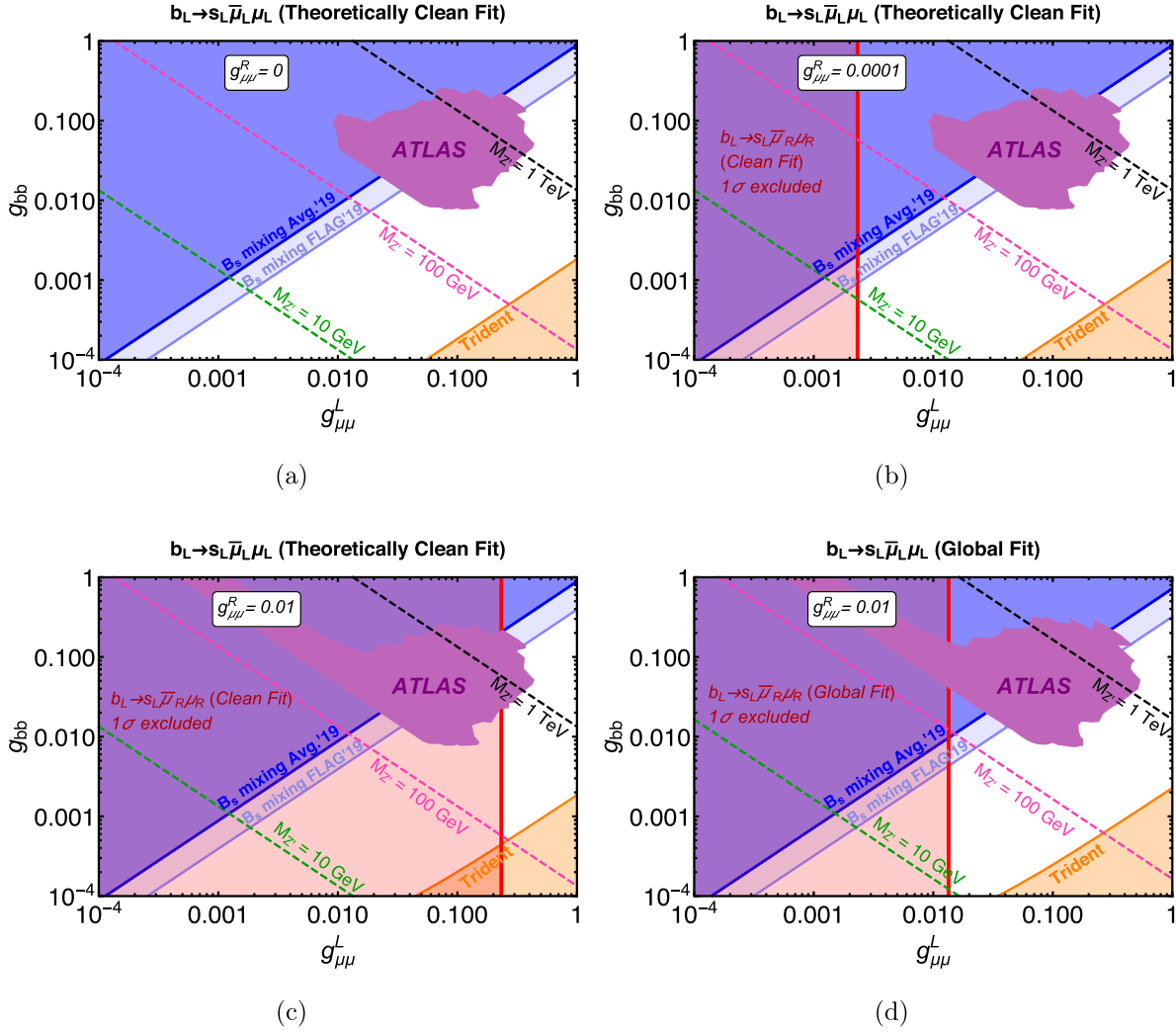


FIG. 3. The parameter space in the  $(g_{\mu\mu}^L, g_{bb})$  plane compatible with  $R_{K^{(*)}}$  anomalies and flavor constraints (white). The  $Z'$  mass varies over the plane, with a unique  $Z'$  mass for each point in the plane as required to match the best fit value for  $G_{bs\mu}^L$  [Eq. (26)] of the theoretically clean fit in Table II [Fig. 3(a), 3(b), 3(c)] and the global fit in Table III [Fig. 3(d)]. We show the recent  $B_s - \bar{B}_s$  mixing constraints (blue and light blue) [78], the neutrino trident bounds (orange) [79], and the region excluded by LHC dimuon resonance searches (purple) [80]. When a nonvanishing  $g_{\mu\mu}^R$  is considered, the red-shaded region is excluded of the  $1\sigma$  range of  $G_{bs\mu}^R$  [Eq. (27)] for the considered fit. The dashed lines correspond to constant values of  $M_{Z'}$  as specified in the plots.

of the  $Z$  decays to four muons, with the second muon pair produced in the SM via a virtual photon [84,85],  $pp \rightarrow Z \rightarrow 4\mu$ , set relevant constraints in the low mass region of  $Z'$  models,  $5 \lesssim M_{Z'} \lesssim 70$  GeV [30,83,86,87]. We avoid such a constraint by keeping  $M_{Z'} > 75$  GeV in our analysis.

For heavier  $Z'$  masses, the strongest constraints come from LHC dimuon resonance searches,  $pp \rightarrow Z' \rightarrow \mu^+\mu^-$ , see also [88,89]. In our model, the  $Z'$  is dominantly produced at the LHC through its coupling to bottom quarks,  $b\bar{b} \rightarrow Z'$ . The cross section  $\sigma(b\bar{b} \rightarrow Z')$  from  $b\bar{b}$  collisions is given for  $g_{bb} = 1$  in Fig. 3 of Ref. [90], we multiply it by  $g_{bb}^2$  in order to obtain the cross section for any  $g_{bb}$ . We neglect a further contribution coming from  $b\bar{s} \rightarrow Z'$  since it is CKM suppressed by  $V_{ts}^2$ . Therefore, we assume that  $\sigma(pp \rightarrow Z')$  is dominated by the subprocess

$b\bar{b} \rightarrow Z'$ . The  $Z'$  boson can subsequently decay into muons, muon neutrinos, bottom quarks, bottom-strange quark pair, and also into top quarks when kinematically allowed. The partial decay widths are given by

$$\begin{aligned}
 \Gamma_{Z' \rightarrow \mu\bar{\mu}} &= \frac{1}{24\pi} [(g_{\mu\mu}^L)^2 + (g_{\mu\mu}^R)^2] M_{Z'}, \\
 \Gamma_{Z' \rightarrow \nu_\mu \bar{\nu}_\mu} &= \frac{1}{24\pi} (g_{\mu\mu}^L)^2 M_{Z'}, \\
 \Gamma_{Z' \rightarrow b\bar{b}} &= \frac{1}{8\pi} g_{bb}^2 M_{Z'}, & \Gamma_{Z' \rightarrow b\bar{s}} &= \frac{1}{8\pi} g_{bb}^2 V_{ts}^2 M_{Z'}, \\
 \Gamma_{Z' \rightarrow t\bar{t}} &= \frac{1}{8\pi} g_{bb}^2 M_{Z'} \left(1 - \frac{m_t^2}{M_{Z'}^2}\right) \sqrt{1 - \frac{4m_t^2}{M_{Z'}^2}}, \quad (40)
 \end{aligned}$$

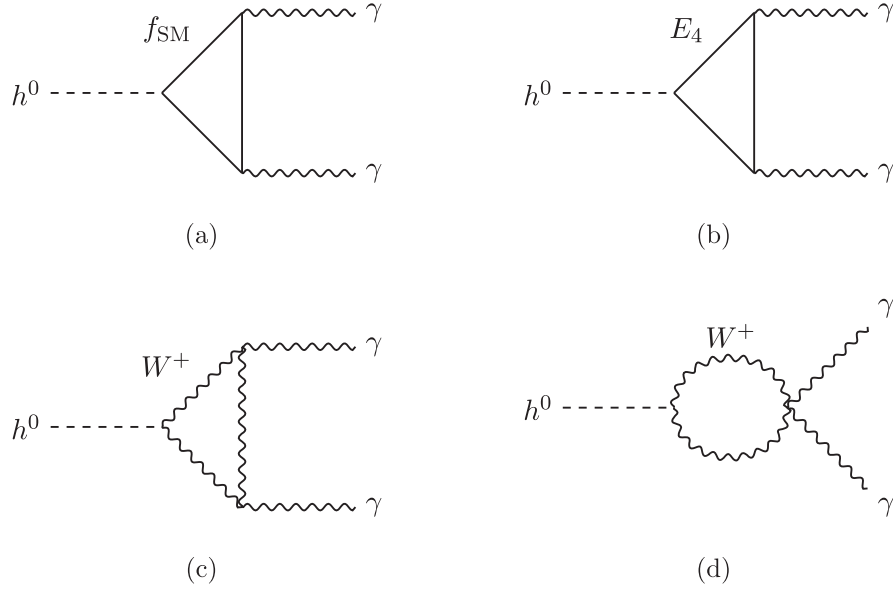


FIG. 4. Diagrams contributing to the Higgs diphoton decay ( $h^0 \rightarrow \gamma\gamma$ ) where  $f_{\text{SM}} = u_i, d_i, e_i, i = 1, 2, 3$  and  $E_4$  is the 4th family VL lepton.

from which we compute  $\text{Br}(Z' \rightarrow \mu\bar{\mu})$  analytically,

$$\text{Br}(Z' \rightarrow \mu\bar{\mu}) = \frac{\Gamma_{Z' \rightarrow \mu\bar{\mu}}}{\Gamma_{Z' \rightarrow \mu\bar{\mu}} + \Gamma_{Z' \rightarrow \nu_\mu \bar{\nu}_\mu} + \Gamma_{Z' \rightarrow b\bar{b}} + \Gamma_{Z' \rightarrow b\bar{s}} + \Gamma_{Z' \rightarrow \bar{t}i}}. \quad (41)$$

Then  $\sigma(pp \rightarrow Z' \rightarrow \mu^+\mu^-)$  is estimated using the narrow-width approximation,

$$\sigma(pp \rightarrow Z' \rightarrow \mu^+\mu^-) \approx \sigma(pp \rightarrow Z') \text{Br}(Z' \rightarrow \mu\bar{\mu}), \quad (42)$$

and compared with the limits obtained from the dimuon resonance search by ATLAS [80], which allows us to constrain  $Z'$  masses between 150 GeV and 5 TeV. Previous studies [30] verified that the analogous Tevatron analyses give weaker constraints than LHC. All things considered, the resulting ATLAS constraints will be shown as purple regions over the parameter space.

### G. Higgs diphoton decay

After spontaneous symmetry breaking (SSB), the Yukawa term in Eq. (4) involving the SM Higgs field and the 4th VL lepton gives rise to the chirality-flipping mass  $M_4^C$ , which gives a very important contribution in Eq. (22) for accommodating  $\Delta a_\mu$  with the experimental measurements. On the other hand,  $M_4^C$  is also expected to give an extra contribution to the decay of the Standard Model Higgs to two photons, a process that has been explored in colliders. Firstly, within the SM, fermions [Fig. 4(a)] and  $W^\pm$  bosons [Figs. 4(c), 4(d)] contribute to the decay channel  $h^0 \rightarrow \gamma\gamma$  [91]

$$\Gamma(h^0 \rightarrow \gamma\gamma)_{\text{SM}} = \frac{\alpha^2 m_h^3}{256\pi^3 v^2} \left| F_1(\tau_W) + \sum_{f \in \text{SM}} N_{cf} Q_f^2 F_{1/2}(\tau_f) \right|^2, \quad (43)$$

where  $\alpha = 1/137$ ,  $m_h = 126$  GeV,  $v = 246$  GeV,  $N_{cf} = 1$  (leptons), 3 (quarks),  $Q_f$  is the electromagnetic charge of the fermion  $f$  in units of  $e$ , and the loop functions are defined as

$$F_1 = 2 + 3\tau + 3\tau(2 - \tau)f(\tau), \quad (44)$$

$$F_{1/2} = -2\tau[1 + (1 - \tau)f(\tau)], \quad (45)$$

with

$$\tau_i = 4m_i^2/m_h^2 \quad (46)$$

and

$$f(\tau) = \begin{cases} [\arcsin(1/\sqrt{\tau})]^2, & \text{if } \tau \geq 1, \\ -\frac{1}{4} \left[ \ln\left(\frac{1+\sqrt{1-\tau}}{1-\sqrt{1-\tau}}\right) - i\pi \right]^2, & \text{if } \tau < 1. \end{cases} \quad (47)$$

Note here that for large  $\tau$ ,  $F_{1/2} \rightarrow -4/3$ . The dominant contribution to  $\Gamma(h^0 \rightarrow \gamma\gamma)_{\text{SM}}$  is the contribution of the  $W$  bosons,

$$F_1(\tau_W) \simeq 8.33, \quad (48)$$

and it interferes destructively with the top-quark loop

$$N_{ct} Q_i^2 F_{1/2}(\tau_f) = 3(2/3)^2(-1.37644) = -1.83526, \quad (49)$$

therefore

$$\begin{aligned} \Gamma(h^0 \rightarrow \gamma\gamma)_{\text{SM}} &= \frac{\alpha^2 m_h^3}{256\pi^3 v^2} |8.33 - 1.83526|^2 \\ &\simeq 9.15636 \times 10^{-6} \text{ GeV}. \end{aligned} \quad (50)$$

The exact result by taking into account the contribution of all SM fermions is

$$\Gamma(h^0 \rightarrow \gamma\gamma)_{\text{SM}} = 9.34862 \times 10^{-6} \text{ GeV}, \quad (51)$$

and if we take  $\Gamma(h^0 \rightarrow \text{all})_{\text{PDG 2021}} = 3.2_{-2.2}^{+2.8}$  MeV, then

$$\text{BR}(h^0 \rightarrow \gamma\gamma)_{\text{SM}} = \frac{\Gamma(h^0 \rightarrow \gamma\gamma)_{\text{SM}}}{\Gamma(h^0 \rightarrow \text{all})_{\text{PDG 2021}}} \times 100 \simeq 0.29\%. \quad (52)$$

Now we add the contribution of a fourth VL lepton [Fig. 4(b)] with VL mass  $M_4^L$  that couples to the Higgs via the chirality-flipping mass  $M_4^C$ , where  $M_4^L \gg M_4^C$  (in such a way that the propagating mass of the fourth lepton can be approximated by the VL mass) [92],

$$\begin{aligned} \Gamma(h^0 \rightarrow \gamma\gamma) &= \frac{\alpha^2 m_h^3}{256\pi^3 v^2} \left| F_1(\tau_W) + \sum_{f \in \text{SM}} N_{cf} Q_f^2 F_{1/2}(\tau_f) \right. \\ &\quad \left. + \frac{M_4^C}{M_4^L} F_{1/2}(\tau_{E_4}) \right|^2. \end{aligned} \quad (53)$$

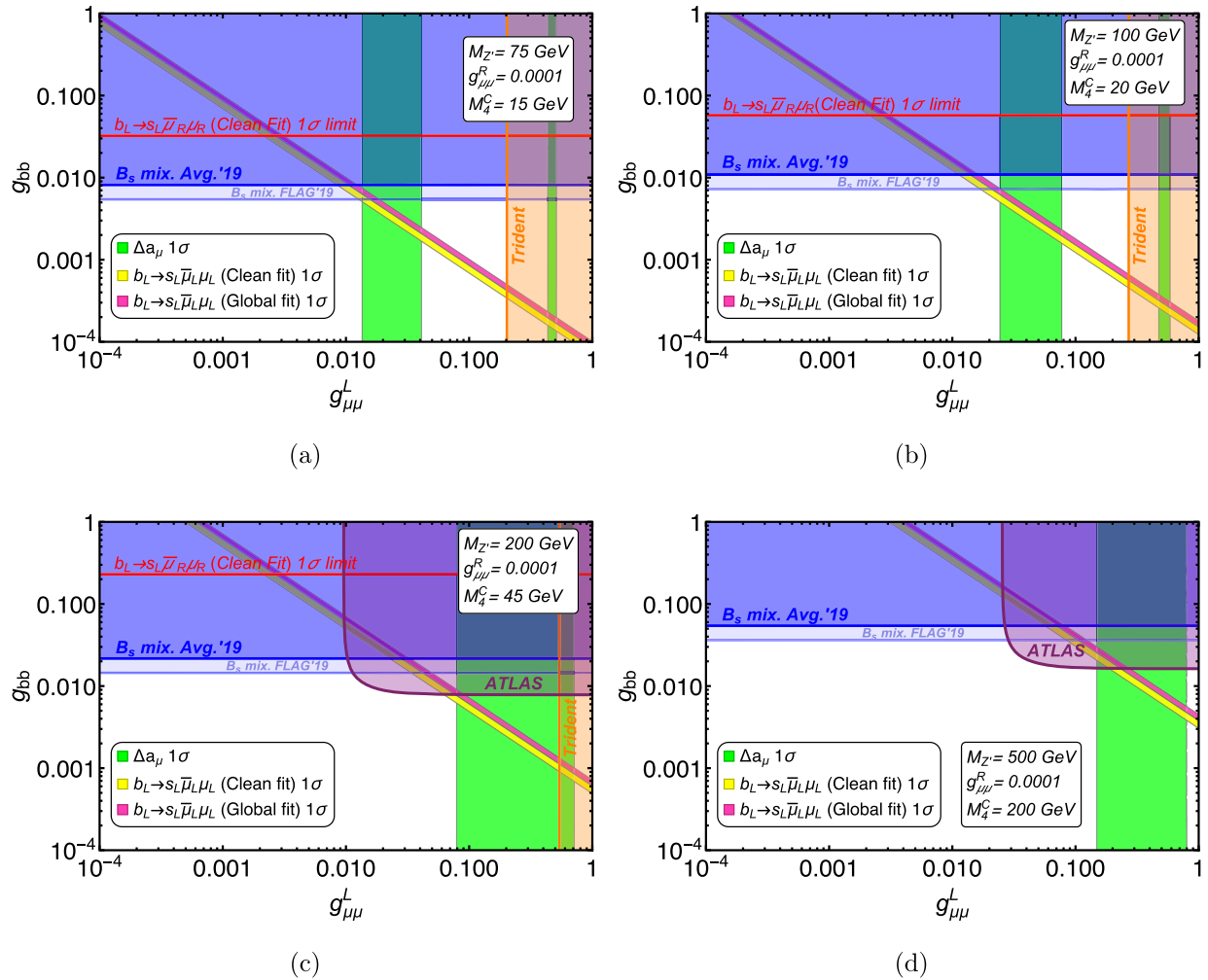


FIG. 5. Bounds on the parameter space in the  $(g_{\mu\mu}^L, g_{bb})$  plane for fixed  $Z'$  masses: 75, 100, 200 and 500 GeV, as indicated on each panel. Each panel also displays the considered  $M_4^C$  and  $g_{\mu\mu}^R$ , while the propagating mass of the VL lepton is always kept as  $m_E \simeq M_4^L = 5$  TeV. The green region explains  $\Delta a_\mu$  up to  $1\sigma$ . The yellow and pink regions fit the Wilson coefficient  $G_{bs\mu}^L$  (26) up to  $1\sigma$  for the theoretically clean fit and the global fit [24], respectively. The red horizontal line shows the limit of the  $1\sigma$  region for the Wilson coefficient  $G_{bs\mu}^R$  (27) in the more restrictive theoretically clean fit (i.e.,  $G_{bs\mu}^R \leq 0.03$ ), in such a way that the parameter space above the red line is excluded. The blue and orange areas show the  $B_s - \bar{B}_s$  mixing [78] and neutrino trident [79] exclusions, respectively, while the purple region is excluded by LHC dimuon resonance searches [80].

We can see that the new contribution proportional to the chirality-flipping mass is suppressed by the heavier VL mass. Moreover, this new contribution decreases  $\Gamma(h^0 \rightarrow \gamma\gamma)$ , since it interferes destructively with the most sizable contribution of the  $W$  bosons. Let us now compare with the experimental results for the  $h^0$  signal strength in the  $h^0 \rightarrow \gamma\gamma$  channel [93],

$$R_{\gamma\gamma} = \frac{\Gamma(h^0 \rightarrow \gamma\gamma)}{\Gamma(h^0 \rightarrow \gamma\gamma)_{\text{SM}}}, \quad (54)$$

$$R_{\gamma\gamma}^{\text{PDG,2020}} = 1.11_{-0.09}^{+0.1}. \quad (55)$$

In the case of  $M_4^C = 200$  GeV,

$$R_{\gamma\gamma}^{\text{VL}} = \frac{|8.33 - 1.83526 - 0.0533333|^2}{|8.33 - 1.83526|^2} = 0.983813. \quad (56)$$

In the case of  $M_4^C = 600$  GeV,

$$R_{\gamma\gamma}^{\text{VL}} = \frac{|8.33 - 1.83526 - 0.16|^2}{|8.33 - 1.83526|^2} = 0.951336. \quad (57)$$

Therefore, even for a value of  $M_4^C$  close to the perturbation theory limit  $M_4^C \lesssim \sqrt{4\pi}v/\sqrt{2} \simeq 616.8$  GeV, the chirality-flipping mass contribution to  $h^0 \rightarrow \gamma\gamma$  is within the  $2\sigma$  range of  $R_{\gamma\gamma}^{\text{PDG,2020}}$ .

## V. RESULTS AND DISCUSSION

In Fig. 3 we have displayed the parameter space in the  $(g_{\mu\mu}^L, g_{bb})$  plane for  $g_{\mu\mu}^R = 0, 0.0001, 0.01$ , considering the theoretically clean fit [Figs. 3(a), 3(b), 3(c)] and the global fit [Fig. 3(d)]. In every case, there is parameter space free from all the constraints that is able to explain  $R_{K^{(*)}}$ . If we set  $g_{\mu\mu}^R = 0$  (Fig. 3(a)), we are making a purely left-handed explanation of  $R_{K^{(*)}}$ , hence recovering the same results as in Ref. [30]. As  $g_{\mu\mu}^R$  is increased, the condition of keeping the contribution to  $b_L \rightarrow s_L \bar{\mu}_R \mu_R$  (namely the Wilson coefficient  $G_{bs\mu}^R$ ) within the  $1\sigma$  range becomes constraining over

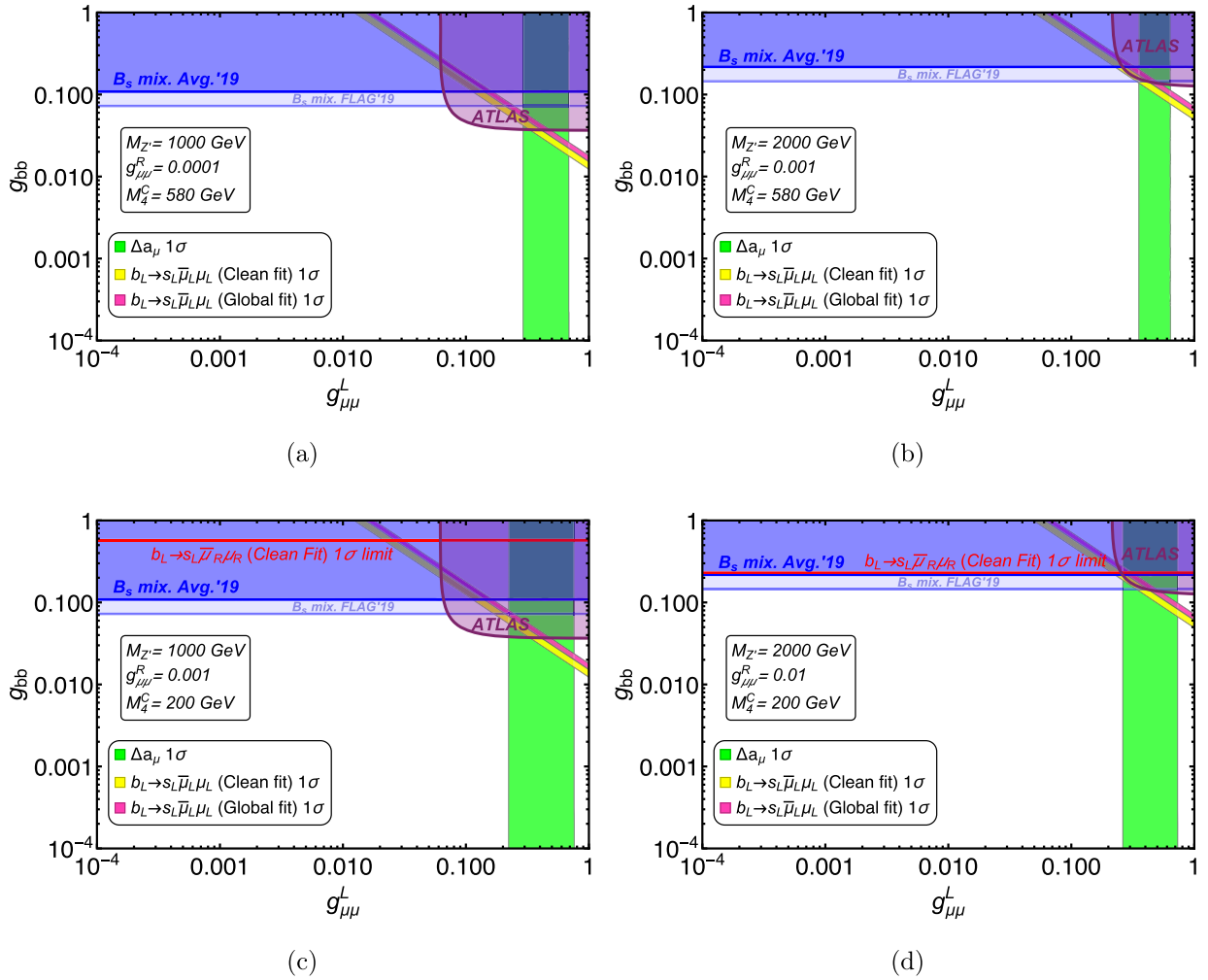


FIG. 6. The same as in Fig. 5 but for heavy  $Z'$  masses: 1000 and 2000 GeV, as indicated on each panel.

the parameter space, especially when the theoretically clean fit is considered [Figs. 3(b), 3(c)]. On the other hand, if the global fit is considered [Fig. 3(d)], then larger values of  $g_{\mu\mu}^R$  are accessible.

In Figs. 5 and 6, for light and heavy  $Z'$  masses respectively, it can be seen that both the contribution to  $b_L \rightarrow s_L \bar{\mu}_L \mu_L$  that explains  $R_{K^{(*)}}$  (namely the Wilson coefficient  $G_{bs\mu}^L$ ) and  $\Delta a_\mu$  can be produced simultaneously within their  $1\sigma$  region by a  $Z'$  with a mass in the range of 75 GeV to 2 TeV, for both the theoretically clean fit and the global fit. Within this range of masses,  $G_{bs\mu}^L$ ,  $G_{bs\mu}^R$  and  $\Delta a_\mu$  can be simultaneously fitted with the same parameters up to the  $1\sigma$  ranges of both the theoretically clean fit and the global fit, since in all the considered cases the parameter space where  $G_{bs\mu}^L$  and  $\Delta a_\mu$  are simultaneously explained is also within the  $1\sigma$  range of  $G_{bs\mu}^R$ . The upper bound for the latter in the theoretically clean fit is displayed in Figs. 5 and 6 as a red horizontal line, there is no lower bound displayed since  $G_{bs\mu}^R$  is compatible with zero in both fits. In all the explored cases, the condition of fitting  $G_{bs\mu}^R$  is less constraining than  $B_s - \bar{B}_s$  mixing.

For light  $Z'$  masses around 75–200 GeV (Fig. 5), both anomalies  $R_{K^{(*)}}$  and  $\Delta a_\mu$  can be explained simultaneously with the condition of small  $g_{\mu\mu}^R$  and  $M_4^C$ . On the other hand, as displayed in Fig. 6, for heavy  $Z'$  masses of 1–2 TeV both anomalies can also be explained simultaneously but it is required to increase either  $g_{\mu\mu}^R$  (two lower panels of Fig. 6) or  $M_4^C$  (two upper panels of Fig. 6). In every case,  $M_4^C$  is kept below the perturbation theory limit of  $M_4^C \lesssim \sqrt{4\pi}v/\sqrt{2} \approx 618$  GeV, and its contribution to Higgs diphoton decay has been previously proven to be within the  $2\sigma$  range of the experimental signals even for values of  $M_4^C$  close to the perturbation theory limit. Moreover, in every case  $g_{\mu\mu}^R$  is set to values for which  $G_{bs\mu}^R$  can be simultaneously fitted, hence  $R_{K^{(*)}}$  is explained. Fitting both anomalies simultaneously for  $M_{Z'} > 2$  TeV could in principle be possible but would require chirality-flipping masses too close to the perturbation theory limit, and/or values of  $g_{\mu\mu}^R$  of  $\mathcal{O}(0.1)$  or higher, for which the  $1\sigma$  range of  $G_{bs\mu}^R$  in the theoretically clean fit becomes more challenging to fit, leading to constraints over the parameter space larger than the present limits of  $B_s - \bar{B}_s$  mixing. Instead, if we consider the global fit that includes angular observables of  $B \rightarrow K^* \bar{\mu} \mu$  data, here  $G_{bs\mu}^R$  is compatible with larger positive values and hence also larger  $g_{\mu\mu}^R$  are accessible, in such a way that explaining both anomalies with heavier masses of  $Z'$  is possible. However, Figs. 5 and 6 also show that collider constraints coming from dimuon resonance searches by ATLAS [80] are very constraining for  $M_{Z'} > 500$  GeV. Although in every case we can still find good points that simultaneously explain both  $R_{K^{(*)}}$  and  $\Delta a_\mu$  while avoiding the ATLAS constraint, such points

could be ruled out in the future by the upcoming LHC run 3 starting in 2022.

## VI. CONCLUSIONS

We have shown that both muon anomalies  $R_{K^{(*)}}$  and  $(g-2)_\mu$  can be simultaneously addressed in a simplified fermiophobic  $Z'$  model with  $75 \text{ GeV} \lesssim M_{Z'} \lesssim 2 \text{ TeV}$ . The explanation of  $(g-2)_\mu$  in this model requires nonvanishing couplings of  $Z'$  to left-handed and right-handed muons  $g_{\mu\mu}^L$ ,  $g_{\mu\mu}^R$ , along with a nonvanishing chirality-flipping mass  $M_4^C$  obtained from the coupling of a fourth vectorlike lepton to the SM Higgs. The explanation of  $R_{K^{(*)}}$  also requires a coupling of  $Z'$  to  $bs$ -quarks. Such  $Z'$  couplings are obtained in this model through mixing of muons and bottom quarks with a fourth vectorlike fermion family. In particular, the  $Z'$  coupling to  $bs$  is CKM suppressed since  $g_{bb}V_{ts}$  in the basis in which the up-quark mass matrix is diagonal.

The scenario considered in this paper represents a minimal mixing framework in which only three mixing parameters are involved. By contrast, other  $Z'$  models that address both muon anomalies are either not fermiophobic [62,63], consider extra symmetries [61] or involve a general mixing framework with a very large number of parameters [64,65], where only a search of best fit points is performed. Instead, within the simplified approach followed here, we had been able to systematically explore the parameter space, extracting interesting conclusions in the process.

The fact that the explanation of the muon  $g-2$  anomaly requires a nonzero coupling  $g_{\mu\mu}^R \neq 0$  means that it is not possible to provide a purely left-handed explanation of  $R_{K^{(*)}}$  as in previous studies [29,30] which do not consider the muon  $g-2$  anomaly. Consequently it is necessary here to fit both the LH and RH Wilson coefficients of the effective operators,  $G_{bs\mu}^L$  and  $G_{bs\mu}^R$ , within the  $1\sigma$  range that explains  $R_{K^{(*)}}$  according to the latest global fits [24]. This leads to a more involved and highly constrained analysis than often considered, which is summarized as follows.

Explaining both muon  $g-2$  and  $R_{K^{(*)}}$  anomalies for  $M_{Z'} > 2$  TeV becomes challenging if we consider the theoretically clean fit where the positive  $1\sigma$  region of  $G_{bs\mu}^R$  is small. This is because larger values of  $g_{\mu\mu}^R$  are required to explain  $(g-2)_\mu$ , but then this implies smaller values of  $g_{bb}$  to keep  $G_{bs\mu}^R$  within the  $1\sigma$  range of the theoretically clean fit. For heavier masses of  $Z'$ , larger values of  $g_{bb}$  are required to fit  $G_{bs\mu}^L$ . However, the heavier the  $Z'$  boson is, the larger the values of  $M_4^C$  must be to explain  $(g-2)_\mu$ , with  $M_4^C$  bounded from above by perturbation theory,  $M_4^C \lesssim \sqrt{4\pi}v/\sqrt{2} \approx 618$  GeV. On the other hand, if we consider the global fit that includes angular observables of  $B \rightarrow K^* \bar{\mu} \mu$  data, here  $G_{bs\mu}^R$  is compatible with larger positive values and hence also larger  $g_{\mu\mu}^R$  are

allowed, but the perturbation theory constraint over  $M_4^C$  remains. Despite these challenges we have been able to find viable regions of parameter space which can explain both the muon  $g-2$  and  $R_{K^{(*)}}$ , for both global fits.

Finally, we have studied the impact of collider searches for this simplified model: constraints coming from experimental measurements of  $Z \rightarrow 4\mu$  can be avoided by keeping  $M_{Z'} > 70$  GeV [30,83,86,87]. However, dimuon resonance searches by ATLAS [80] are already very constraining for  $M_{Z'} > 500$  GeV, in such a way that the

good results of this model for heavy  $Z'$  masses could be probed by the upcoming LHC run 3 starting in 2022.

## ACKNOWLEDGMENTS

This project has received funding from the European Union's Horizon 2020 Research and Innovation programme under Marie Skłodowska-Curie grant agreement HIDDeN European ITN project (No. H2020-MSCA-ITN-2019//860881-HIDDeN). S. F. K. acknowledges the STFC Consolidated Grant No. ST/L000296/1.

- 
- [1] J. P. Lees *et al.* (BABAR Collaboration), Measurement of branching fractions and rate asymmetries in the rare decays  $B \rightarrow K^{(*)}l^+l^-$ , *Phys. Rev. D* **86**, 032012 (2012).
- [2] S. Choudhury *et al.* (BELLE Collaboration), Test of lepton flavor universality and search for lepton flavor violation in  $B \rightarrow K\ell\ell$  decays, *J. High Energy Phys.* **03** (2021) 105.
- [3] R. Aaij *et al.* (LHCb Collaboration), Test of Lepton Universality Using  $B^+ \rightarrow K^+\ell^+\ell^-$  Decays, *Phys. Rev. Lett.* **113**, 151601 (2014).
- [4] R. Aaij *et al.* (LHCb Collaboration), Search for Lepton-Universality Violation in  $B^+ \rightarrow K^+\ell^+\ell^-$  Decays, *Phys. Rev. Lett.* **122**, 191801 (2019).
- [5] R. Aaij *et al.* (LHCb Collaboration), Test of lepton universality in beauty-quark decays, [arXiv:2103.11769](https://arxiv.org/abs/2103.11769).
- [6] R. Aaij *et al.* (LHCb Collaboration), Test of lepton universality with  $B^0 \rightarrow K^{*0}\ell^+\ell^-$  decays, *J. High Energy Phys.* **08** (2017) 055.
- [7] S. Descotes-Genon, L. Hofer, J. Matias, and J. Virto, Global analysis of  $b \rightarrow s\ell\ell$  anomalies, *J. High Energy Phys.* **06** (2016) 092.
- [8] C. Bobeth, G. Hiller, and G. Piranishvili, Angular distributions of  $\bar{B} \rightarrow \bar{K}\ell^+\ell^-$  decays, *J. High Energy Phys.* **12** (2007) 040.
- [9] M. Bordone, G. Isidori, and A. Pattori, On the Standard Model predictions for  $R_K$  and  $R_{K^*}$ , *Eur. Phys. J. C* **76**, 440 (2016).
- [10] D. M. Straub, flavio: A PYTHON package for flavour and precision phenomenology in the Standard Model and beyond, [arXiv:1810.08132](https://arxiv.org/abs/1810.08132).
- [11] G. Isidori, S. Nabeebaccus, and R. Zwicky, QED corrections in  $\bar{B} \rightarrow \bar{K}\ell^+\ell^-$  at the double-differential level, *J. High Energy Phys.* **12** (2020) 104.
- [12] G. Hiller and I. Nisandzic,  $R_K$  and  $R_{K^*}$  beyond the standard model, *Phys. Rev. D* **96**, 035003 (2017).
- [13] M. Ciuchini, A. M. Coutinho, M. Fedele, E. Franco, A. Paul, L. Silvestrini, and M. Valli, On flavourful easter eggs for new physics hunger and lepton flavour universality violation, *Eur. Phys. J. C* **77**, 688 (2017).
- [14] L.-S. Geng, B. Grinstein, S. Jäger, J. Martin Camalich, X.-L. Ren, and R.-X. Shi, Towards the discovery of new physics with lepton-universality ratios of  $b \rightarrow s\ell\ell$  decays, *Phys. Rev. D* **96**, 093006 (2017).
- [15] B. Capdevila, A. Crivellin, S. Descotes-Genon, J. Matias, and J. Virto, Patterns of new physics in  $b \rightarrow s\ell^+\ell^-$  transitions in the light of recent data, *J. High Energy Phys.* **01** (2018) 093.
- [16] D. Ghosh, Explaining the  $R_K$  and  $R_{K^*}$  anomalies, *Eur. Phys. J. C* **77**, 694 (2017).
- [17] D. Bardhan, P. Byakti, and D. Ghosh, Role of tensor operators in  $R_K$  and  $R_{K^*}$ , *Phys. Lett. B* **773**, 505 (2017).
- [18] S. L. Glashow, D. Guadagnoli, and K. Lane, Lepton Flavor Violation in  $B$  Decays? *Phys. Rev. Lett.* **114**, 091801 (2015).
- [19] G. D'Amico, M. Nardecchia, P. Panci, F. Sannino, A. Strumia, R. Torre, and A. Urbano, Flavour anomalies after the  $R_{K^*}$  measurement, *J. High Energy Phys.* **09** (2017) 010.
- [20] L. Calibbi, A. Crivellin, and T. Ota, Effective Field Theory Approach to  $b \rightarrow s\ell\ell^{(\prime)}$ ,  $B \rightarrow K^{(*)}\nu\bar{\nu}$  and  $B \rightarrow D^{(*)}\tau\nu$  with Third Generation Couplings, *Phys. Rev. Lett.* **115**, 181801 (2015).
- [21] J. Aebischer, W. Altmannshofer, D. Guadagnoli, M. Reboud, P. Stangl, and D. M. Straub,  $B$ -decay discrepancies after Moriond 2019, *Eur. Phys. J. C* **80**, 252 (2020).
- [22] A. Carvunis, F. Dettori, S. Gangal, D. Guadagnoli, and C. Normand, On the effective lifetime of  $B_s \rightarrow \mu\mu\gamma$ , *J. High Energy Phys.* **12** (2021) 078.
- [23] A. Angelescu, D. Bečirević, D. A. Faroughy, F. Jaffredo, and O. Sumensari, On the single leptoquark solutions to the  $B$ -physics anomalies, *Phys. Rev. D* **104**, 055017 (2021).
- [24] L.-S. Geng, B. Grinstein, S. Jäger, S.-Y. Li, J. Martin Camalich, and R.-X. Shi, Implications of new evidence for lepton-universality violation in  $b \rightarrow s\ell^+\ell^-$  decays, *Phys. Rev. D* **104**, 035029 (2021).
- [25] A. Crivellin, G. D'Ambrosio, and J. Heeck, Explaining  $h \rightarrow \mu^+\tau^+$ ,  $B \rightarrow K^*\mu^+\mu^-$  and  $B \rightarrow K\mu^+\mu^-/B \rightarrow Ke^+e^-$  in a Two-Higgs-Doublet Model with Gauged  $L_\mu - L_\tau$ , *Phys. Rev. Lett.* **114**, 151801 (2015).
- [26] A. Crivellin, G. D'Ambrosio, and J. Heeck, Addressing the LHC flavor anomalies with horizontal gauge symmetries, *Phys. Rev. D* **91**, 075006 (2015).
- [27] C.-W. Chiang, X.-G. He, J. Tandean, and X.-B. Yuan,  $R_{K^{(*)}}$  and related  $b \rightarrow s\ell\ell$  anomalies in minimal flavor violation framework with  $Z'$  boson, *Phys. Rev. D* **96**, 115022 (2017).

- [28] S. F. King, Flavourful  $Z'$  models for  $R_{K^{(*)}}$ , *J. High Energy Phys.* **08** (2017) 019.
- [29] S. F. King,  $R_{K^{(*)}}$  and the origin of Yukawa couplings, *J. High Energy Phys.* **09** (2018) 069.
- [30] A. Falkowski, S. F. King, E. Perdomo, and M. Pierre, Flavourful  $Z'$  portal for vector-like neutrino dark matter and  $R_{K^{(*)}}$ , *J. High Energy Phys.* **08** (2018) 061.
- [31] D. Bečirević and O. Sumensari, A leptoquark model to accommodate  $R_K^{\text{exp}} < R_K^{\text{SM}}$  and  $R_{K^*}^{\text{exp}} < R_{K^*}^{\text{SM}}$ , *J. High Energy Phys.* **08** (2017) 104.
- [32] I. de Medeiros Varzielas and S. F. King,  $R_{K^{(*)}}$  with leptoquarks and the origin of Yukawa couplings, *J. High Energy Phys.* **11** (2018) 100.
- [33] I. de Medeiros Varzielas and S. F. King, Origin of Yukawa couplings for Higgs bosons and leptoquarks, *Phys. Rev. D* **99**, 095029 (2019).
- [34] S. F. King, Twin Pati-Salam theory of flavour with a TeV scale vector leptoquark, *J. High Energy Phys.* **11** (2021) 161.
- [35] G. W. Bennett *et al.* (Muon  $g-2$  Collaboration), Final report of the muon E821 anomalous magnetic moment measurement at BNL, *Phys. Rev. D* **73**, 072003 (2006).
- [36] B. Abi *et al.* (Muon  $g-2$  Collaboration), Measurement of the Positive Muon Anomalous Magnetic Moment to 0.46 ppm, *Phys. Rev. Lett.* **126**, 141801 (2021).
- [37] T. Aoyama *et al.*, The anomalous magnetic moment of the muon in the Standard Model, *Phys. Rep.* **887**, 1 (2020).
- [38] T. Aoyama, M. Hayakawa, T. Kinoshita, and M. Nio, Complete Tenth-Order QED Contribution to the Muon  $g-2$ , *Phys. Rev. Lett.* **109**, 111808 (2012).
- [39] T. Aoyama, T. Kinoshita, and M. Nio, Theory of the anomalous magnetic moment of the electron, *Atoms* **7**, 28 (2019).
- [40] A. Czarnecki, W. J. Marciano, and A. Vainshtein, Refinements in electroweak contributions to the muon anomalous magnetic moment, *Phys. Rev. D* **67**, 073006 (2003); Erratum, *Phys. Rev. D* **73**, 119901 (2006).
- [41] C. Gnendiger, D. Stöckinger, and H. Stöckinger-Kim, The electroweak contributions to  $(g-2)_\mu$  after the Higgs boson mass measurement, *Phys. Rev. D* **88**, 053005 (2013).
- [42] M. Davier, A. Hoecker, B. Malaescu, and Z. Zhang, Reevaluation of the hadronic vacuum polarisation contributions to the Standard Model predictions of the muon  $g-2$  and  $\alpha(m_Z^2)$  using newest hadronic cross-section data, *Eur. Phys. J. C* **77**, 827 (2017).
- [43] A. Keshavarzi, D. Nomura, and T. Teubner, Muon  $g-2$  and  $\alpha(M_Z^2)$ : A new data-based analysis, *Phys. Rev. D* **97**, 114025 (2018).
- [44] G. Colangelo, M. Hoferichter, and P. Stoffer, Two-pion contribution to hadronic vacuum polarization, *J. High Energy Phys.* **02** (2019) 006.
- [45] M. Hoferichter, B.-L. Hoid, and B. Kubis, Three-pion contribution to hadronic vacuum polarization, *J. High Energy Phys.* **08** (2019) 137.
- [46] M. Davier, A. Hoecker, B. Malaescu, and Z. Zhang, A new evaluation of the hadronic vacuum polarisation contributions to the muon anomalous magnetic moment and to  $\alpha(m_Z^2)$ , *Eur. Phys. J. C* **80**, 241 (2020); Erratum, *Eur. Phys. J. C* **80**, 410 (2020).
- [47] A. Keshavarzi, D. Nomura, and T. Teubner,  $g-2$  of charged leptons,  $\alpha(M_Z^2)$ , and the hyperfine splitting of muonium, *Phys. Rev. D* **101**, 014029 (2020).
- [48] A. Kurz, T. Liu, P. Marquard, and M. Steinhauser, Hadronic contribution to the muon anomalous magnetic moment to next-to-next-to-leading order, *Phys. Lett. B* **734**, 144 (2014).
- [49] K. Melnikov and A. Vainshtein, Hadronic light-by-light scattering contribution to the muon anomalous magnetic moment revisited, *Phys. Rev. D* **70**, 113006 (2004).
- [50] P. Masjuan and P. Sanchez-Puertas, Pseudoscalar-pole contribution to the  $(g_\mu - 2)$ : A rational approach, *Phys. Rev. D* **95**, 054026 (2017).
- [51] G. Colangelo, M. Hoferichter, M. Procura, and P. Stoffer, Dispersion relation for hadronic light-by-light scattering: Two-pion contributions, *J. High Energy Phys.* **04** (2017) 161.
- [52] M. Hoferichter, B.-L. Hoid, B. Kubis, S. Leupold, and S. P. Schneider, Dispersion relation for hadronic light-by-light scattering: Pion pole, *J. High Energy Phys.* **10** (2018) 141.
- [53] A. Gérardin, H. B. Meyer, and A. Nyffeler, Lattice calculation of the pion transition form factor with  $N_f = 2 + 1$  Wilson quarks, *Phys. Rev. D* **100**, 034520 (2019).
- [54] J. Bijnens, N. Hermansson-Truedsson, and A. Rodríguez-Sánchez, Short-distance constraints for the HLbL contribution to the muon anomalous magnetic moment, *Phys. Lett. B* **798**, 134994 (2019).
- [55] G. Colangelo, F. Hagelstein, M. Hoferichter, L. Laub, and P. Stoffer, Longitudinal short-distance constraints for the hadronic light-by-light contribution to  $(g-2)_\mu$  with large- $N_c$  Regge models, *J. High Energy Phys.* **03** (2020) 101.
- [56] T. Blum, N. Christ, M. Hayakawa, T. Izubuchi, L. Jin, C. Jung, and C. Lehner, Hadronic Light-by-Light Scattering Contribution to the Muon Anomalous Magnetic Moment from Lattice QCD, *Phys. Rev. Lett.* **124**, 132002 (2020).
- [57] G. Colangelo, M. Hoferichter, A. Nyffeler, M. Passera, and P. Stoffer, Remarks on higher-order hadronic corrections to the muon  $g-2$ , *Phys. Lett. B* **735**, 90 (2014).
- [58] W. Altmannshofer, C.-Y. Chen, P. S. Bhupal Dev, and A. Soni, Lepton flavor violating  $Z'$  explanation of the muon anomalous magnetic moment, *Phys. Lett. B* **762**, 389 (2016).
- [59] A. E. Cárcamo Hernández, S. F. King, H. Lee, and S. J. Rowley, Is it possible to explain the muon and electron  $g-2$  in a  $Z'$  model?, *Phys. Rev. D* **101**, 115016 (2020).
- [60] G. Bélanger, C. Delaunay, and S. Westhoff, A dark matter relic from muon anomalies, *Phys. Rev. D* **92**, 055021 (2015).
- [61] A. E. Cárcamo Hernández, S. Kovalenko, R. Pasechnik, and I. Schmidt, Phenomenology of an extended IDM with loop-generated fermion mass hierarchies, *Eur. Phys. J. C* **79**, 610 (2019).
- [62] B. Allanach, F. S. Queiroz, A. Strumia, and S. Sun,  $Z'$  models for the LHCb and  $g-2$  muon anomalies, *Phys. Rev. D* **93**, 055045 (2016); Erratum, *Phys. Rev. D* **95**, 119902 (2017).
- [63] S. Raby and A. Trautner, Vectorlike chiral fourth family to explain muon anomalies, *Phys. Rev. D* **97**, 095006 (2018).

- [64] J. Kawamura, S. Raby, and A. Trautner, Complete vectorlike fourth family and new  $U(1)'$  for muon anomalies, *Phys. Rev. D* **100**, 055030 (2019).
- [65] J. Kawamura, S. Raby, and A. Trautner, Complete vectorlike fourth family with  $U(1)'$ : A global analysis, *Phys. Rev. D* **101**, 035026 (2020).
- [66] J. Kawamura and S. Raby, Signal of four muons or more from a vector-like lepton decaying to a muon-philic  $Z'$  boson at the LHC, *Phys. Rev. D* **104**, 035007 (2021).
- [67] K.-m. Cheung, Muon anomalous magnetic moment and leptoquark solutions, *Phys. Rev. D* **64**, 033001 (2001).
- [68] E. Coluccio Leskow, G. D'Ambrosio, A. Crivellin, and D. Müller,  $(g-2)_\mu$ , lepton flavor violation, and  $Z$  decays with leptoquarks: Correlations and future prospects, *Phys. Rev. D* **95**, 055018 (2017).
- [69] A. Crivellin, D. Mueller, and F. Saturnino, Correlating  $h\mu + \mu^-$  to the Anomalous Magnetic Moment of the Muon via Leptoquarks, *Phys. Rev. Lett.* **127**, 021801 (2021).
- [70] P. Arnan, A. Crivellin, M. Fedele, and F. Mescia, Generic loop effects of new scalars and fermions in  $b \rightarrow s\ell^+\ell^-$ ,  $(g-2)_\mu$  and a vector-like 4th generation, *J. High Energy Phys.* **06** (2019) 118.
- [71] A. Crivellin, M. Hoferichter, and P. Schmidt-Wellenburg, Combined explanations of  $(g-2)_{\mu,e}$  and implications for a large muon EDM, *Phys. Rev. D* **98**, 113002 (2018).
- [72] A. Crivellin and M. Hoferichter, Consequences of chirally enhanced explanations of  $(g-2)_\mu$  for  $h \rightarrow \mu\mu$  and  $Z \rightarrow \mu\mu$ , *J. High Energy Phys.* **07** (2021) 135.
- [73] A. E. C. Hernández, S. F. King, and H. Lee, Fermion mass hierarchies from vectorlike families with an extended 2HDM and a possible explanation for the electron and muon anomalous magnetic moments, *Phys. Rev. D* **103**, 115024 (2021).
- [74] R. Bause, G. Hiller, T. Höhne, D. F. Litim, and T. Stuedtner, B-Anomalies from flavorful  $U(1)'$  extensions, safely, *Eur. Phys. J. C* **82**, 42 (2022).
- [75] R. H. Parker, C. Yu, W. Zhong, B. Estey, and H. Müller, Measurement of the fine-structure constant as a test of the Standard Model, *Science* **360**, 191 (2018).
- [76] L. Morel, Z. Yao, P. Cladé, and S. Guellati-Khélifa, Determination of the fine-structure constant with an accuracy of 81 parts per trillion, *Nature (London)* **588**, 61 (2020).
- [77] J. Hernandez-Garcia and S. F. King, New Weinberg operator for neutrino mass and its seesaw origin, *J. High Energy Phys.* **05** (2019) 169.
- [78] L. Di Luzio, M. Kirk, A. Lenz, and T. Rauh,  $\Delta M_s$  theory precision confronts flavour anomalies, *J. High Energy Phys.* **12** (2019) 009.
- [79] A. Falkowski, M. González-Alonso, and K. Mimouni, Compilation of low-energy constraints on 4-fermion operators in the SMEFT, *J. High Energy Phys.* **08** (2017) 123.
- [80] M. Aaboud *et al.* (ATLAS Collaboration), Search for new high-mass phenomena in the dilepton final state using  $36 \text{ fb}^{-1}$  of proton-proton collision data at  $\sqrt{s} = 13 \text{ TeV}$  with the ATLAS detector, *J. High Energy Phys.* **10** (2017) 182.
- [81] D. Geiregat *et al.* (CHARM-II Collaboration), First observation of neutrino trident production, *Phys. Lett. B* **245**, 271 (1990).
- [82] S. R. Mishra *et al.* (CCFR Collaboration), Neutrino Tridents and  $WZ$  Interference, *Phys. Rev. Lett.* **66**, 3117 (1991).
- [83] W. Altmannshofer, S. Gori, M. Pospelov, and I. Yavin, Neutrino Trident Production: A Powerful Probe of New Physics with Neutrino Beams, *Phys. Rev. Lett.* **113**, 091801 (2014).
- [84] S. Chatrchyan *et al.* (CMS Collaboration), Observation of  $Z$  decays to four leptons with the CMS detector at the LHC, *J. High Energy Phys.* **12** (2012) 034.
- [85] G. Aad *et al.* (ATLAS Collaboration), Measurements of Four-Lepton Production at the  $Z$  Resonance in  $pp$  Collisions at  $\sqrt{s} = 7$  and  $8 \text{ TeV}$  with ATLAS, *Phys. Rev. Lett.* **112**, 231806 (2014).
- [86] W. Altmannshofer, S. Gori, M. Pospelov, and I. Yavin, Quark flavor transitions in  $L_\mu - L_\tau$  models, *Phys. Rev. D* **89**, 095033 (2014).
- [87] W. Altmannshofer, S. Gori, S. Profumo, and F. S. Queiroz, Explaining dark matter and  $B$  decay anomalies with an  $L_\mu - L_\tau$  model, *J. High Energy Phys.* **12** (2016) 106.
- [88] M. Abdullah, M. Dalchenko, B. Dutta, R. Eusebi, P. Huang, T. Kamon, D. Rathjens, and A. Thompson, Bottom-quark fusion processes at the LHC for probing  $Z'$  models and  $B$ -meson decay anomalies, *Phys. Rev. D* **97**, 075035 (2018).
- [89] R. Alonso, P. Cox, C. Han, and T. T. Yanagida, Flavoured  $B - L$  local symmetry and anomalous rare  $B$  decays, *Phys. Lett. B* **774**, 643 (2017).
- [90] D. A. Faroughy, A. Greljo, and J. F. Kamenik, Confronting lepton flavor universality violation in  $B$  decays with high- $p_T$  tau lepton searches at LHC, *Phys. Lett. B* **764**, 126 (2017).
- [91] J. F. Gunion, H. E. Haber, G. L. Kane, and S. Dawson, The Higgs Hunter's Guide, *Front. Phys.* **80**, 1 (2000), <https://inspirehep.net/literature/279039>.
- [92] N. Bizot and M. Frigerio, Fermionic extensions of the Standard Model in light of the Higgs couplings, *J. High Energy Phys.* **01** (2016) 036.
- [93] P. A. Zyla *et al.* (Particle Data Group), Review of particle physics, *Prog. Theor. Exp. Phys.* (2020), 083C01.